sustainability

MDPI

Article

Study of the Mechanical Properties and Water Stability of Microbially Cured, Coir-Fiber-Reinforced Clay Soil

Qizhi Hu [1,2], Wensen Song [1,*] and Jianwen Hu [1]

[1] School of Civil Architecture and Environment, Hubei University of Technology, Wuhan 430068, China
[2] Hubei Bridge Safety Monitoring Technology and Equipment Technology Engineering Research Center, Wuhan 430068, China
* Correspondence: 102100794@hbut.edu.cn

Abstract: Clay soil is widely distributed in engineering foundations. Because of its poor stability, low load-bearing capacity, and poor water stability, it does not provide a high-quality foundation. Microbial-induced calcium carbonate precipitation (MICP) is a novel soil consolidation technique. The basic principle of this technique is that microorganisms induce calcium carbonate deposition in the soil, solidifying it. The reinforcement treatment of clayey soil via MICP with fiber reinforcement can make full use of the advantages of both techniques to improve the mechanical properties and water stability of the soil. In this study, in order to facilitate engineering applications, bacillus pasteurii liquid was mixed with coconut-fiber-reinforced soil using the mixing method, and a microbial solidification test was carried out on the reinforced clayey soil with fiber contents of 0, 0.2%, 0.4%, and 0.6% (mass ratio). By conducting triaxial consolidation without a drainage test, the calcium carbonate content determination test and the disintegration test were combined with SEM microscopic image analysis to compare and analyze the mechanical properties and water stability of clayey soil under different fiber treatments. The results show the following: (1) The coupling of the two techniques can effectively improve the shear strength of the soil. The shear strength first increased and then decreased with the increase in the fiber content. The optimum fiber content is 0.4%, and the shear strength is 120% higher than that of plain soil. (2) The addition of fiber significantly increased the cohesive force of the clayey soil. In addition, the friction angle was also increased by the synergistic effect of the fiber and calcium carbonate. The cohesive force was increased in the range of 3.2~24.4 kPa, and the internal friction angle was increased in the range of 2.2°~6.4°. (3) As the fiber content increased, the disintegration resistance of the solidified soil was obviously improved, and the disintegration rate decreased with the increase in fiber content. When the fiber content was 0.6%, the final disintegration rate was the lowest. (4) Fiber reinforcement increased the colonization space of the microorganisms and improved the deposition efficiency and yield of the calcium carbonate, and the cementing effect of the calcium carbonate promoted fiber reinforcement.

Keywords: microbial curing; fiber reinforcement; coconut fiber; triaxial test; water stability

Citation: Hu, Q.; Song, W.; Hu, J. Study of the Mechanical Properties and Water Stability of Microbially Cured, Coir-Fiber-Reinforced Clay Soil. *Sustainability* **2023**, *15*, 13261. https://doi.org/10.3390/su151713261

Academic Editors: Md. Mizanur Rahman and Castorina Silva Vieira

Received: 1 August 2023
Revised: 16 August 2023
Accepted: 1 September 2023
Published: 4 September 2023

1. Introduction

As a class of soil that is widely distributed in China, clayey soil is a medium–soft soil type. Its disadvantages, such as poor stability, low load-bearing capacity, and poor water stability, have caused difficulties in engineering construction in coastal areas. Traditional soil reinforcement methods, such as the large mechanical compaction method and the chemical grouting method, generally consume a large amount of energy and have long construction periods and high costs. Furthermore, mechanical compaction disturbs the soil and destroys its original structure, while chemical grouting often pollutes the soil and is thus not environmentally friendly. Therefore, the research and development of technology that has low energy consumption and green-curing abilities could hold significant promise.

In recent years, the technology of microbial-induced calcium carbonate precipitation (MICP) has attracted a great deal of attention because of its simple, clean, and efficient construction; it is a biochemical mineralization process, which occurs inside the soil. Bacteria can adsorb the Ca^{2+} in the solution on environmental species cell surfaces. Moreover, urea decomposes into ${CO_3}^{2-}$ and ${NH_4}^{1+}$, and Ca^{2+} combines with ${CO_3}^{2-}$ to produce a large number of calcium carbonate crystals on a cell's surface. The large amount of calcium carbonate that is generated on the surface of the bacteria distributed throughout the soil bonds the soil micro-particles and fills the internal pores and fissures of the material, thus improving the physical and mechanical properties of the soil. The chemical formula of the reaction is as follows [1]:

$$Ca^{2+} + Cell \rightarrow Cell - Ca^{2+}, \tag{1}$$

$$NH_2 - CO - NH_2 + H_2O \xrightarrow{\text{Urease}} 2NH_4^+ + CO_3^{2+}, \tag{2}$$

$$CO_3^{2+} + Cell - Ca^{2+} \rightarrow Cell - CaCO_3. \tag{3}$$

Whiffin et al. first used MICP technology to solidify loose sand and improve its macroscopic mechanical properties [1]. Chu, J. et al. and Qabany et al. tested the curing effect of MICP technology on sand by carrying out mechanical tests [2,3]. Hanlong Liu et al. carried out a field test based on MICP technology on an island in the South China Sea, and the results showed that the surface strength of the calcareous sand foundation strengthened by MICP was significantly improved, with a good overall effect [4]. Mingjuan Cui et al. carried out a series of studies on the effects of different chemical treatment methods and particle sizes on microbial solidification, and they analyzed the influence of various factors on the mechanical properties of MICP-modified soil [5,6]. Stocks-Fischer et al. found that the number, size, and morphology of calcium carbonate crystals were different at different temperatures and pH values [7,8]. Wang et al. found that when the bacterial buds were placed in a neutral (pH = 7) or weakly alkaline (pH = 9.1) environment, the urea decomposition rate reached more than 90%, while in a strong alkaline environment (pH = 12.5), the rate was only 5% [9]. Xiaohui Cheng et al. used microbial solidification technology to reinforce a liquefied sand foundation and studied its dynamic characteristics [10]. In a study of red–brown basalt residual soil, Yanrui Chen et al. found that the shear strength of the soil was significantly improved after microbial solidification [11]. The effectiveness of MICP technology in improving clayey soil was verified by John Xie et al., who used it to improve the water stability of clayey soil [12]. The disintegration of microbially improved loess was discussed by Tianchi Xu et al. [13]. Lu Liu et al. used the method of microbial solidification to treat dams. The anti-erosion ability of the dam was improved after surface treatment [14]. Xiaojun Liu et al. discussed the application of MICP technology to the repair and solidification of fissures in earthen sites [15]. The effect of MICP on the mechanical properties of calcareous sand was investigated by Hao Li et al. [16]. Through penetration and scour tests, they found that the MICP-FR synergistic curing technique significantly improved the structural strength and erosion resistance of calcareous sand. De Muynck et al. used bacillus and calcium salt solutions to treat concrete using the soaking method; they found that, as the calcium source, $CaCl_2$ had a better treatment effect [17]. Willem De Muynck et al. used Bacillus sphaericus to induce the formation of calcium carbonate precipitation, which significantly improved the permeability resistance, freeze resistance, and carbonization resistance of cement mortar [17]. Xiaolu Yuan studied the protective enhancement effect of microbial mineralization on cement-based materials by using the bacterial solution soaking method. The strength of cement samples was improved after soaking with the bacterial solution, and the adaptability of the thioaluminate cement base to microbial mineralization was better [18]. P. Gosh et al. mixed shewanella into cement mortar, and the fibrous filling that was formed improved the pore structure of the cement mortar, thus significantly increasing the compressive strength of the specimen [19]. Yu Ding et al. discussed the constitutive model and the damage evolution law of a fiber-reinforced vegetated concrete substrate, providing a theoretical reference for the accurate analysis and evaluation of the mechanical properties of the substrate [20]. Van Tittelboom et al. injected a gel-immobilized bacterial suspension into concrete cracks to improve the repair effect of cracks [21].

Although the strength of the solidified soil has been seen to be improved by MICP technology, it has weak deformation resistance and poor toughness, and, to a large extent, it is a typical brittle material; therefore, the strength is lost instantly after damage and there are certain safety risks involved in using it in construction. Fiber reinforcement is a technology that has emerged in recent years; the addition of fiber has a restraining effect on the soil deformation caused by external loads and limits the development of damaged surfaces and fissures so as to improve the engineering properties of the soil. Many scholars have conducted research on this matter. Jianlong Liu et al. conducted unconfined compressive strength tests with different reinforcement amounts, reinforcement lengths, and reinforcement methods. They determined the optimal fiber content and studied the effect of the reinforcement method on the soil [22]. Liangyong Li et al. used coir shell fiber to strengthen red clay foundations, and the research results provided a reference for the selection of foundation-strengthening materials and foundation strengthening in the Hainan region of China [23]. Wei Xu et al. reinforced soil–cement with glass fiber and studied the influence of the fiber on the durability and water stability of the soil–cement [24]. Bo Pan et al. studied the effects of palm fiber on the shear strength and deformation resistance of vegetated concrete under dry and wet cycles, providing a necessary scientific basis for improving the long-term stability of vegetated concrete substrates [25]. Jianzhuang Xiao et al. found that the addition of sisal fiber can effectively improve the fracture performance of recycled aggregate concrete [26]. Zhenlin Qin et al. discussed the influence of sisal fiber and glass powder on the mechanical properties of concrete [27]. Jianbin Hao et al. studied the effect and mechanism of fly-ash–sisal fiber composite that improved expansive soil, and provided reference for the design and construction of expansive soil subgrade engineering and slope protection engineering [28]. Junjie Zheng's team found that the addition of fiber can improve the toughness and strength of microbial solidified soil [29,30]. Sai Li et al. studied the effect of corn silk fiber on the shear strength of microbial solidified sludge [31]. John Xie et al. found that adding different amounts of fiber to microbially solidified sand can, to varying degrees, improve the strength of the soil [32]. Junling Liang et al. studied the effects of carbon fiber reinforcement and sand particle shapes on the mechanical properties of microbially solidified sand [33]. Choi et al. and Li et al. improved the brittle damage properties of microbially cured soil using the reinforcement technique and discussed the effect of the fiber content on the soil [34,35]. Guo Cheng et al. explored the internal mechanism of the mechanical properties and strength growth of solidified purple soil under different fiber contents and different grouting times [36]. These examples show that the combination of the fiber reinforcement technique and the microbial-induced calcium carbonate deposition technique can be used to improve the strength and toughness of soil.

In order to study the mechanical properties and water stability of microbially solidified soil with the addition of fiber, coconut shell fiber was added into clayey soil using the mixing method, and the soil was solidified with a bacterial liquid. The addition of natural coconut shell fiber alleviates the brittleness of soil caused by the MICP technology, and the synergistic effect of the two technologies also improves the water stability of soil, thereby improving its erosion resistance. The effect of different fiber contents on the shear strength of the solidified soil was studied via a triaxial consolidated undrained shear test of the microbially solidified reinforced soil. The effect of the fiber content on its disintegration rate was investigated with a disintegration test. The coupling mechanism of MICP technology and the fiber reinforcement technology was analyzed through the determination of the calcium carbonate content and through SEM electron microscopy tests. Their effectiveness and applicability are discussed in this paper to provide a reference for the application of the two technologies in soil reinforcement of areas with clayey soil.

2. Experimental Materials and Methods

2.1. Experimental Materials

2.1.1. Clayey Soil and Fiber

The soil used in the test was taken from a site in Jingmen, Hubei, three meters underground. The soil samples were reddish brown and yellowish brown. The soil quality was not uniform. The basic physical indexes of the soil were measured in the laboratory: the moisture content of the soil was measured by the drying method, the density of the soil was measured by the ring knife method and the dry density of the soil was calculated. The liquid plastic limit of the soil was measured by the liquid plastic limit combined measurement method, and other required data were calculated according to the formula. Its basic physical properties are shown in Table 1 below. Compared with synthetic fibers that are used as reinforcing materials, natural fibers are clean, easy to obtain and in line with the concept of green development. Therefore, natural fibers are preferred when selecting reinforced materials. The fibers selected for the test were coconut shell fibers, which were purchased from a fiber processing plant in Hainan. The details are shown in Figure 1 below. The diameter of fibers is 100–500 μm, their length is 5–30 mm, and their density is 1.25 g/cm^3. China is rich in coconut shell resources; therefore, coconut shell fibers cost less than those of other plants that have limited planting areas and complex processing technologies. As agricultural and forestry waste, coconut shells are easy to obtain and only a simple extraction process is required. After processing, coconut shell fibers have high strength and toughness, high elongation at breakage, and are clean and environmentally friendly. These features make them a good reinforcing material [37–39].

Table 1. Physical indices of remolded clayey soil.

Water Content	Dry Density	Void Ratio	Liquid Limit	Plastic Limit	Plasticity Index	Liquidity Index	Modulus of Compression
19%	1.66 g/cm^3	0.722	29.5%	15%	14.5	0.10	6.7 MPa

Figure 1. Coconut shell fibers.

2.1.2. Preparation of the Microbial Culture and Cementation Solution

The bacterium selected for the test was Bacillus pasteurii (ATCC11859), purchased from the Shanghai Conservation Biotechnology Center; this bacterium has no negative impact on the soil environment and has a high urease secretion capacity and activity. It is now widely used in geotechnical engineering. The strain form was a lyophilized powder and was cultured with a liquid medium. Each liter of the liquid medium contained caso agar + urea, 20 g; pepton from casein, 15 g; pepton from soymeal, 5 g; Nacl, 5 g; Agar, 20 g; ddH_20, 900 mL; and was adjusted with 1 mol, NaOH, with a PH value of 7.3, making the medium alkaline [40]. The strain and the medium composed of bacterial broth were placed in a thermostatic shaking incubator and incubated aerobically, at a constant temperature of 30 °C for 36 h, at 200 r/min. The OD600 value of the bacterial broth was tested at 1.472 using a spectrophotometer.

The cementation solution provided the calcium and nitrogen sources and the nutrients required for the microbial curing process, which are usually a mixture of calcium chloride and urea. The cementation solution used in this experiment was a mixture of $CaCl_2$ and urea. The concentration of the cementation solution has different effects on the cementing effect, and studies have shown that an overly high concentration of the cementation solution inhibits microbial activity and reduces the efficiency of calcium carbonate synthesis, thus affecting the curing effect [40]. Therefore, the cementation solution used in this experiment contained 0.5 mol/L urea and 0.5 mol/L $CaCl_2$, mixed in equal volumes.

2.2. Experimental Protocol

In order to determine the most suitable curing method, a pre-test was conducted, and the grouting method was first used for curing [41,42]. As the filling times increased, it became difficult to introduce the solution into the soil, and a large amount of soil flowed out of the upper opening with the solution, making it difficult to cement. After that, the soaking method was used. It was found that the soil sample softened after mold removal, which was difficult to use in practical engineering [43]. In order to improve the uniformity of the spatial distribution of the liquid bacteria and cementation solution in the soil, and to facilitate engineering applications, the test was conducted using the mixing method, and the best moisture content of the clayey soil was determined to be 17%. The water required for the optimal moisture content was replaced by the bacterial liquid and the cementation solution, and a cylindrical specimen 39.1 mm in diameter and 80 mm in height was made according to test specifications. The maximum dry density of the clayey soil is 1.66 g/cm^3, and it was calculated that we required 160 g of soil. The required fiber was weighed and thoroughly mixed with the soil, and then 13.6 g of bacterial liquid was added and left for 3 h, so that the bacterial liquid would be fully attached to the soil; it was then evenly mixed with 13.6 g of the cementation solution. It was necessary to weigh each layer of the clayey soil after mixing it uniformly, in four layers, for manual compaction. Each layer was compacted 30 times. The contact surface between the layers scraping the hairs made good specimens when kept at 30 °C, humidity of 95 ± 2%, for 14 days. The test considered the effect of the fiber content on the shear strength and deformation characteristics of the microbially cured soil. We tested three different fiber contents: 0.2%, 0.4%, and 0.6%, (mass ratio), using the mixing method for curing tests. To avoid chance errors, three parallel tests were conducted for each group of tests.

2.3. Test Methodology

2.3.1. Triaxial Test

The consolidation undrained test was carried out using the TSZ-2 automatic triaxial apparatus (produced by Nanjing Soil Instrument Factory CO., Ltd., Nanjing, China) and the data were collected by the supporting data acquisition system. The device is shown in Figure 2. The accuracy was 0.01 kn for the axial force, 0.01 mm for the axial displacement, and 0.001 mL for the inlet and outlet water and volume deformation. In order to study the effect of the fiber admixture on the microbially cured soil, each group was set up with test conditions of 50 kPa, 100 kPa, and 200 kPa net perimeter pressure for testing. The specimens were vacuum saturated before the test and were solidified and stabilized before we sheared the soil samples. They were sheared at a rate of 0.05 mm/min to 20% of the axial strain to obtain the curve of deviator stress $(\sigma_1 - \sigma_3)_f$ and axial strain (ε).

Figure 2. TSZ-2 fully automatic triaxial instrument.

2.3.2. Calcium Carbonate Content Measurement Test

In the process of reinforcement, only calcium carbonate deposition was generated. Therefore, the amount of calcium carbonate was determined using the acid washing method. First, the specimens with the best fiber content after completing the loading damage were dried and pounded to increase the contact area of the soil so that the calcium carbonate could be more easily dissolved in the acidic solution. After drying again, 20 g of the soil sample was put into a beaker, and an excess of 2 mol/L hydrochloric acid was added and soaked until no bubbles were generated. To make the reaction more complete, the soil sample was left for 24 h, and then the mixture was introduced into a funnel containing filter paper and rinsed three to five times with deionized water. The remaining residue, together with the filter paper, was dried at 105 °C to a constant mass. The amount of calcium carbonate produced (C) was calculated as follows [44]:

$$C = \frac{M_{S+C} - M_S}{M_{S+C}} \times 100\% - C_0, \quad (4)$$

where M_{S+C} is the drying mass of the soil sample before acid washing, 20 g; M_s is the drying mass of the soil sample after acid washing; and C_0 is the initial calcium carbonate content of the clayey soil, 3.1%.

2.3.3. Disintegration Test

To evaluate the water stability of the clayey soil after microbial curing and the fiber reinforcement treatment, disintegration tests were carried out on the specimens. A home-made disintegration apparatus was used, and the device is shown in Figure 3. The test device consisted of a high-precision electronic balance (accuracy of 0.01 g), a disintegration tank, a disintegration box, a stand, a timer, and other parts. The appropriate size of the disintegrating tank and disintegrating box was customized according to the requirements; the size of the metal mesh hole at the bottom of the disintegration box was 1 cm × 1 cm, and the thin wire connected between the disintegration box and the bracket could be freely removed and hung up. The disintegrating box was connected to the bracket with a thin wire and suspended in the disintegrating tank, which was placed on a high-precision electronic balance. Before the test, the disintegration tank was filled with an appropriate amount of water. The specimen was placed in the disintegration box and was lowered slowly into the water after the balance readings remained unchanged. Balance readings were recorded every 30 s, and, according to the rapidity of the disintegration of the specimen, an appropriate adjustment was made to the time interval of the measurement. The disintegration rate of the specimen was calculated using the following formula [13]:

$$P(Tx) = \frac{M(Tx) - M_0}{M_s}, \quad (5)$$

where P (Tx) is the disintegration rate; M_s is the reading of the balance after the complete disintegration of the specimen; M_0 is the reading of the balance when the specimen is completely immersed in water and has not started to disintegrate; and $M(Tx)$ is the reading of the balance at the moment of T.

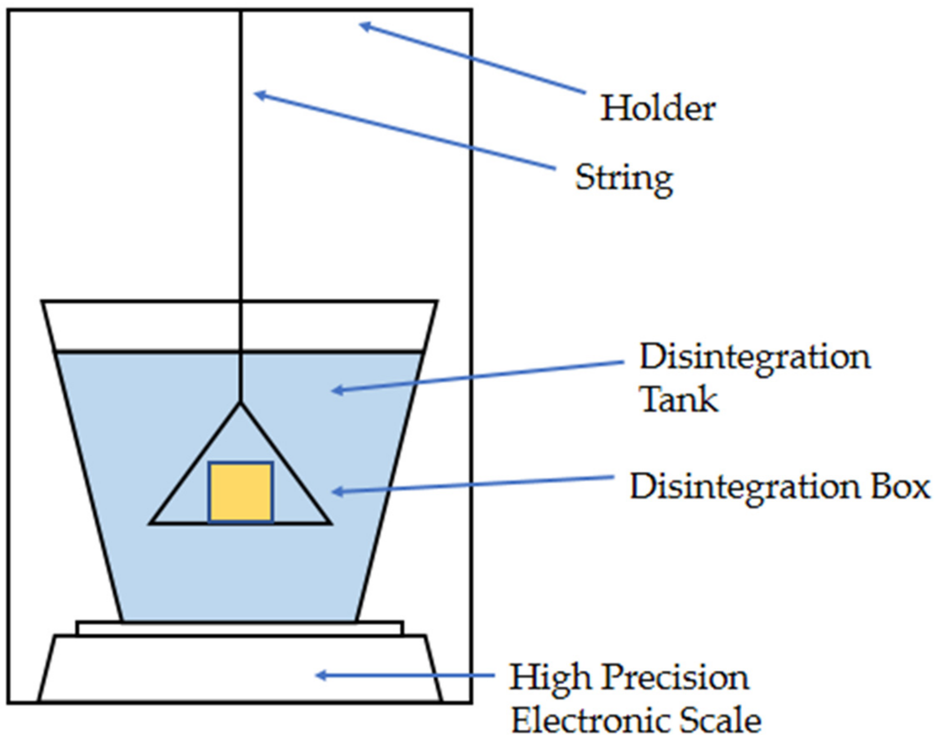

Figure 3. Self-made disintegration instrument.

3. Experimental Results and Analysis

3.1. Triaxial Compression: Test Results and Analysis

3.1.1. Stress–Strain Relationship

The representative curves of the relationship between the axial strain and the principal stress of the fiber-reinforced microbially solidified soil are shown below. Figures 4–7 show the stress–strain relationship curves of the coconut-shell-fiber-reinforced, microbial-cured soil under the conditions of certain fiber contents and different confining pressures. Figures 8–10 show the stress–strain relationship of the microorganisms under the same confining pressure and different fiber contents.

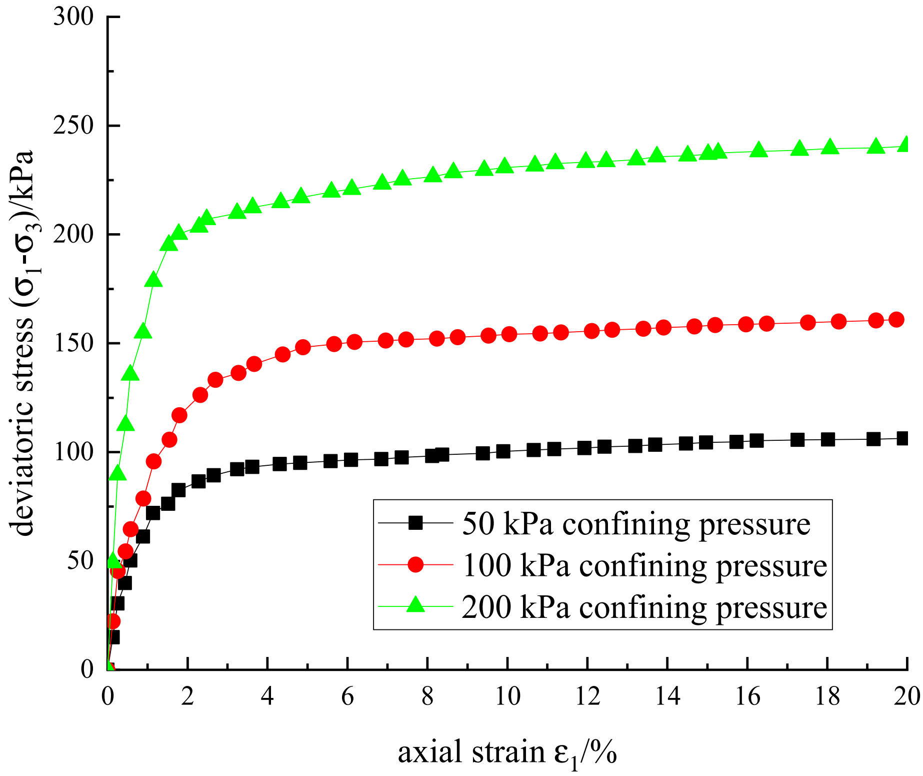

Figure 4. Stress–strain relationship under different confining pressures, with 0% fiber content.

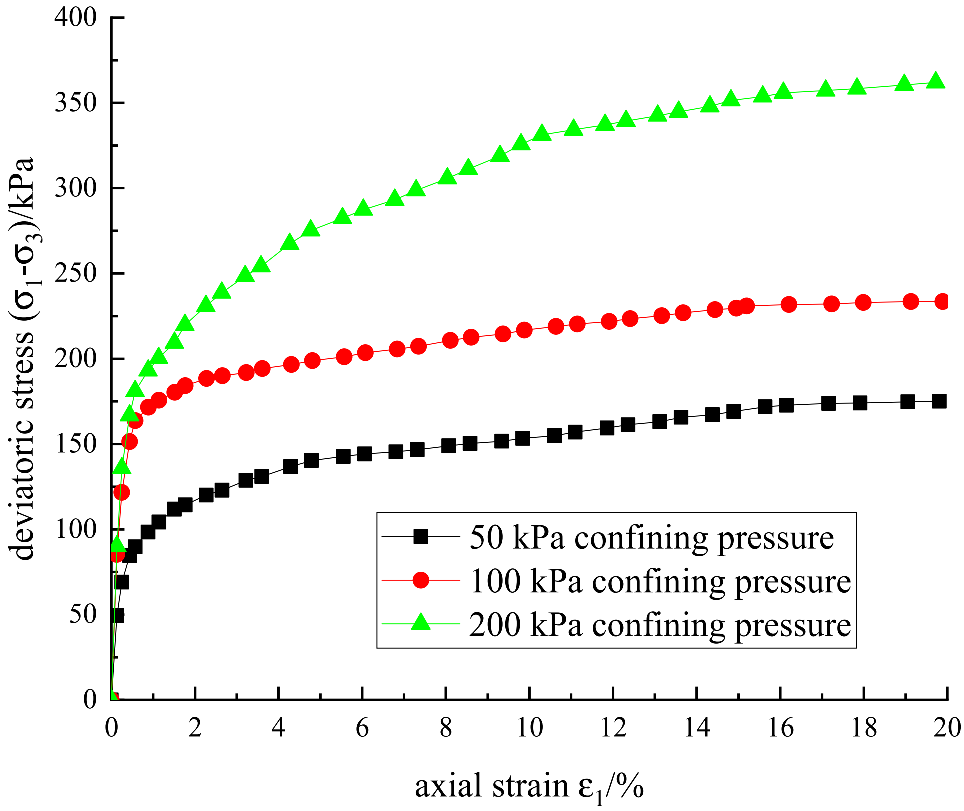

Figure 5. Stress–strain relationship under different confining pressures, with 0.2% fiber content.

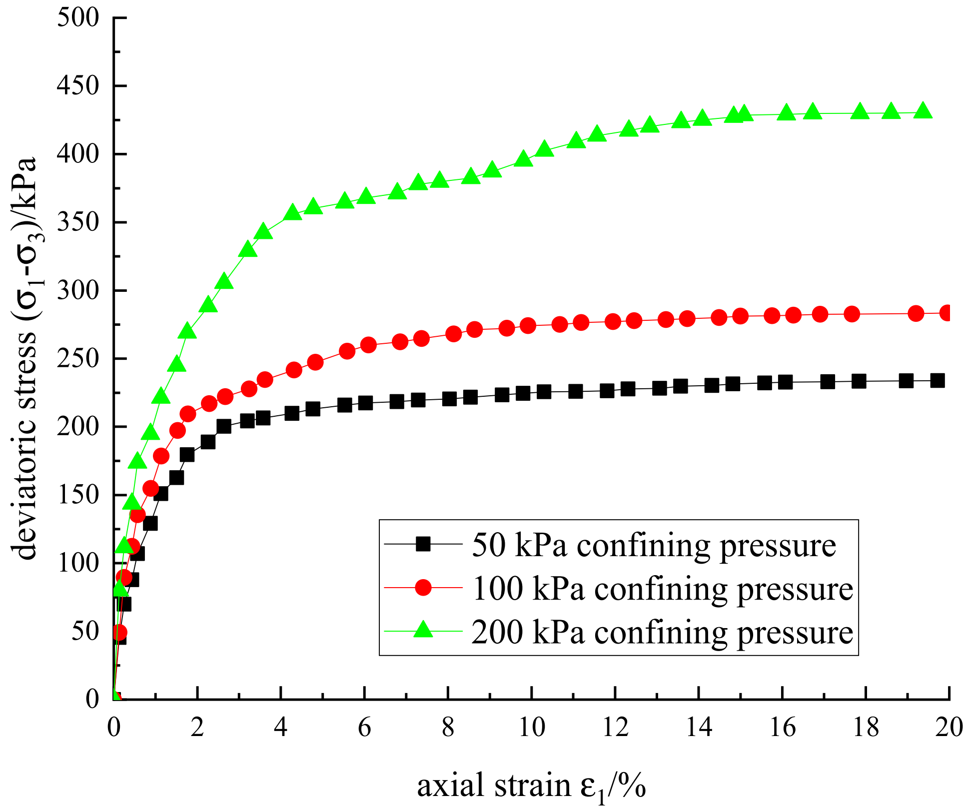

Figure 6. Stress–strain relationship under different confining pressures, with 0.4% fiber content.

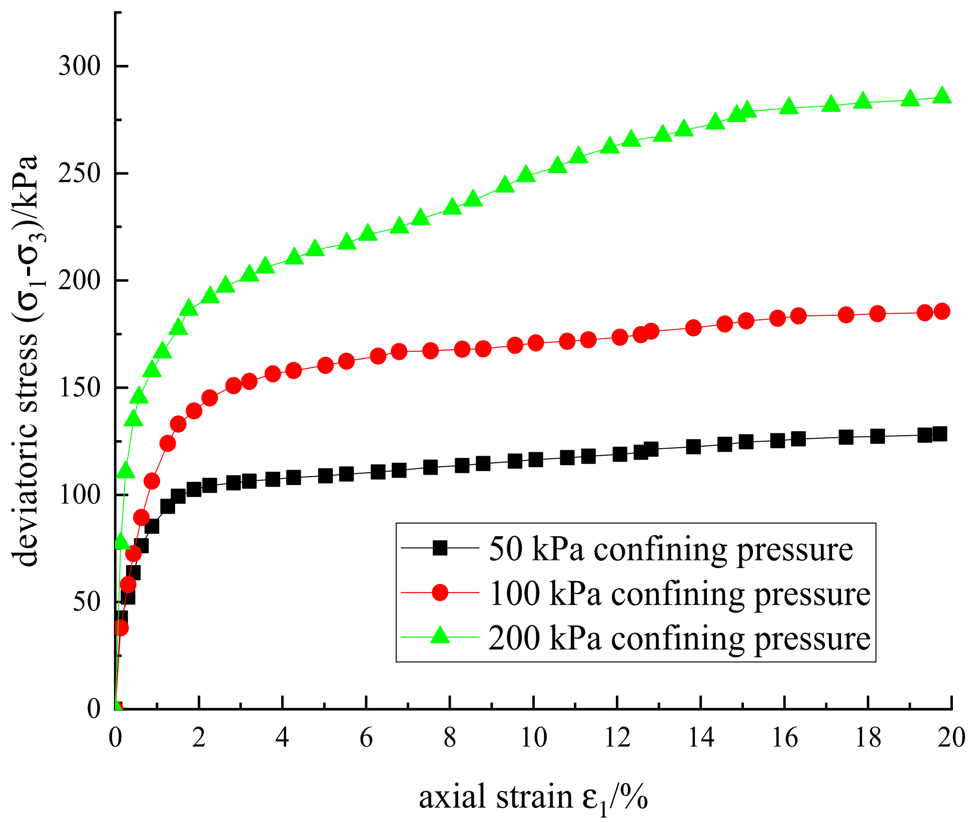

Figure 7. Stress–strain relationship under different confining pressures, with 0.6% fiber content.

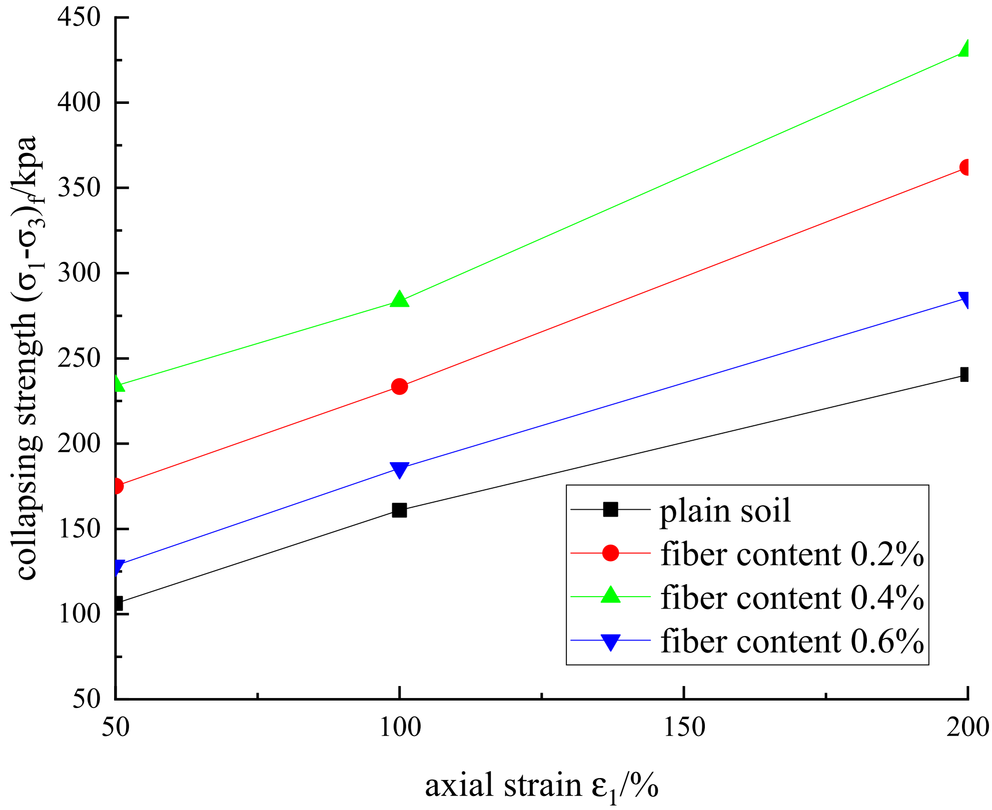

Figure 8. The curve of the change in failure strength with the confining pressure.

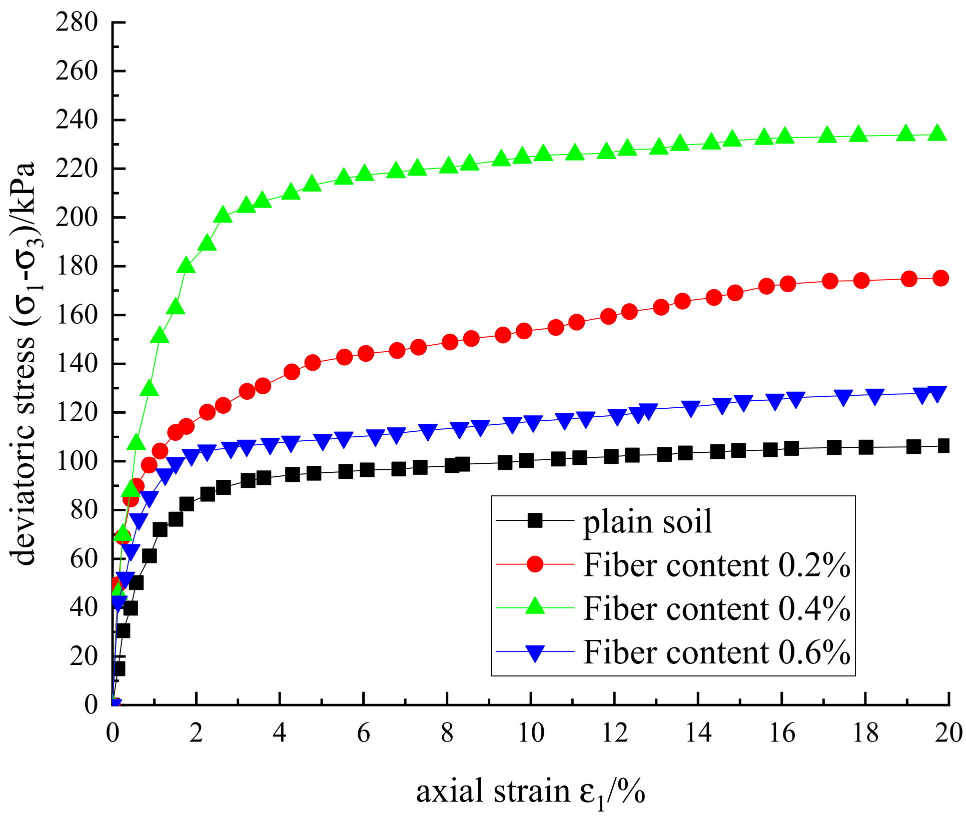

Figure 9. Stress–strain relationship under a confining pressure of 50 kPa and different fiber contents.

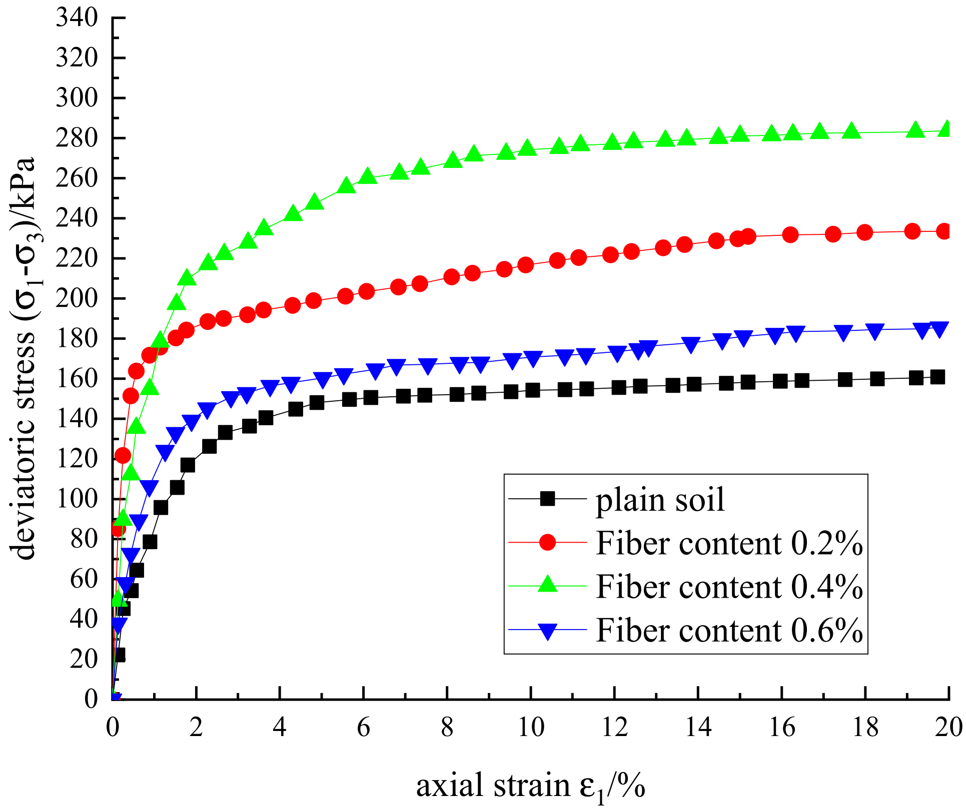

Figure 10. Stress–strain relationship under a confining pressure of 100 kPa and different fiber contents.

Figures 4–7 show that the deviatoric stress of the microbially cured, coconut-shell-fiber-reinforced clayey soil increased gradually with the increase in the confining pressure when the fiber content was certain. When the axial strain was small, under different confining pressures, the stress–strain of the microbially cured plain soil and the fiber-reinforced cured soil basically overlapped, and the initial compressive strength of each specimen was approximately equal; therefore, the reinforcing effect of the fiber was not fully realized. With the increase in the axial strain, the distance between the deviatoric stress and the axial strain curves of the samples under different confining pressures gradually widened and increased, and, after a certain strain (not more than 3%), the increase gradually decreased. Finally, the curve became essentially stable. The curve generally shows a weak hardening type, and the strength of the soil increases with the increase in the axial strain. With the increase in fiber content, the failure strength of the soil increases first and then decreases under a certain confining pressure. An excessive amount of fiber leads to a poor reinforcement effect, and the microbial curing effect is also affected by excessive fiber content. Under certain strains, the main stress difference of the fiber-reinforced cured soil was greater than that of the MICP-cured specimens. This was because the MICP technology induced calcium carbonate crystals, which filled the spaces between the pores of the larger soil particles and played a cementing role, gluing the coconut shell fiber and soil particles into a whole. The microbially induced calcium carbonate deposits were attached to the fiber surface, which made it rougher and improved the bite force between the fiber surface and the soil. The fibers also created more pores in the soil, with calcium carbonate deposits. The fiber acted like an anchor in the soil, strengthening the curing effect of the MICP technique and limiting the displacement and deformation of the soil particles.

Figure 8 shows the variation curve of the breaking strength under the perimeter pressure. The failure strength of the soil was positively correlated with the confining pressure. Under the same confining pressure, the breaking strength of the four different fiber contents in the cured soil, in descending order, were as follows: fiber content 0.4% cured soil > fiber content 0.2% cured soil > fiber content 0.6% cured soil > MICP bacterium-liquid-cured plain soil. Compared to the plain soil that was cured with the bacterial liquid only, the breaking strength of the various reinforced soils increased by 64.7%, 120%, and 20.7%, respectively, according to the fiber content when the perimeter pressure was 50 KPa; the breaking strength of various reinforced soils increased by 45.1%, 76.3%, and 15.3%, respectively, according to the fiber content when the perimeter pressure was 100 KPa; the breaking strength of the various reinforced soils increased by 50.5%, 79%, and 18.7%, respectively, according to the fiber admixture when the perimeter pressure was 200 KPa.

Figures 9–11 show that the form of the triaxial test curve under different fiber doping values still exhibited a trend of strain hardening. The main stress difference increased as the fiber doping values increased and then decreased. The maximum damage strength was achieved at the fiber doping value of 0.4%, which indicated that there is an optimal value of fiber doping; therefore, more is not better, and the reinforced soil strength reaches its maximum when the optimal value is used. For the specimens with the optimum fiber doping value, the strength was increased by 120%, 76.2%, and 79% at σ3 = 50, 100, and 200 kPa, respectively, compared to the plain soil cured by the bacterial liquid. Figure 12 shows that the failure strength of the soil increased first and then decreased with the increase in the fiber content. When the fiber content in the soil is low, it is difficult for the fiber to form a network structure inside the specimen; thus, the interaction with the soil is not sufficient and the reinforcing effect is limited. As the fiber content increases, the fiber distribution is more uniform, the spacing is reduced and it is easier to form a network. This can form a good uniform random support system inside the soil; thus, the cohesion between the soil particles and the fiber increases, which improves the reinforcing effect of the fiber. However, when the fiber content is too high, the fibers easily form into clumps in the mixing process, which reduces the friction and cohesion between the soil particles and weakens the reinforcing effect, resulting in a specimen with lower strength.

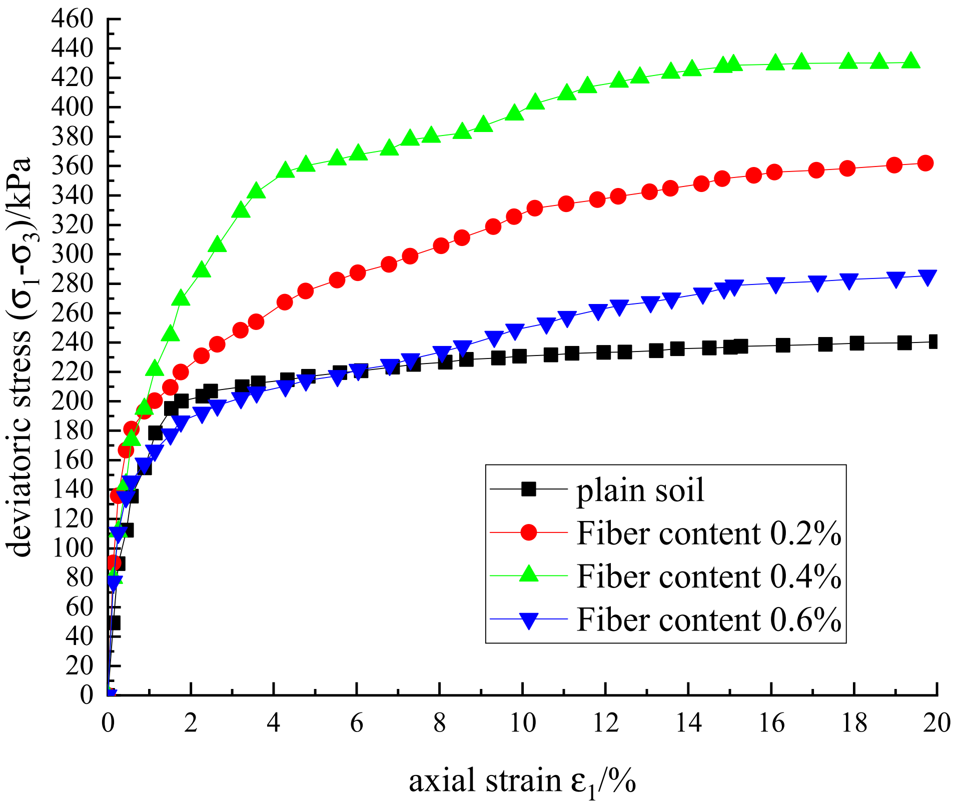

Figure 11. Strain–strain relationship under a confining pressure of 200 kPa different fiber contents.

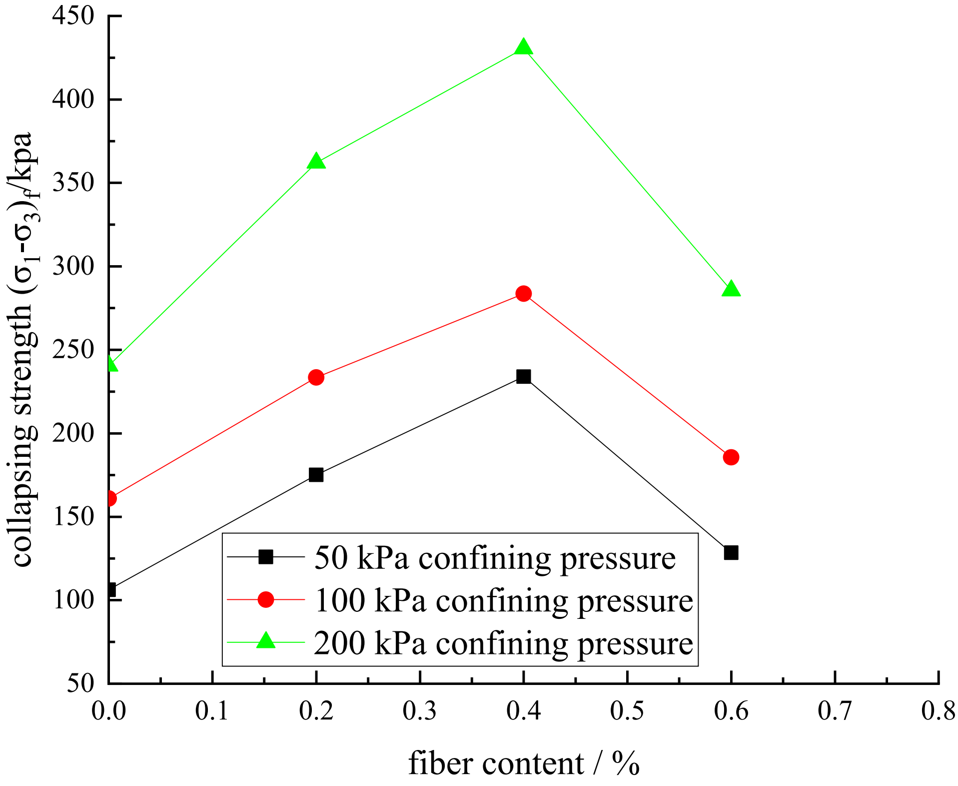

Figure 12. Curve of the change in failure strength with fiber content.

3.1.2. Strength Characteristic Analysis

According to the triaxial test results of the microbial-solidified, coconut-fiber-reinforced clayey soil, the Mohr circle of the specimen was plotted and the common tangent was made for the Mohr circle for the same admixture at different envelope pressures. By using the Mohr–Coulomb theory, the effective stress–shear strength expression $\tau = \sigma \tan \varphi' + c'$ and the effective stress–strength index of the specimen under each doping amount can be calculated (internal friction angle, φ' and cohesion, c'). The specific results are shown in Table 2.

Table 2. Strength index of the coconut-fiber-reinforced, microbially cured soil.

Fiber Content	Cohesion, c'	Angle of Internal Friction, φ'
Plain soil	24.2	17.8
Fiber content 0.2%	36.9	22.6
Fiber content 0.4%	48.6	24.2
Fiber content 0.6%	27.4	20.0

From the shear strength index of the fiber-reinforced microbial-solidified soil shown in Table 2, it can be seen that the shear strength index of the fiber-reinforced, microbial-solidified soil was significantly improved compared with that of the plain soil, which was only solidified by microorganisms. Specifically, the cohesive force of the reinforced soil increased by 3.2~24.4 kPa compared with that of the plain soil, and the cohesive force increased first and then decreased with the increase in the amount of fiber admixture. The effective cohesive force of the reinforced cured soil reached its maximum when the fiber admixture was 0.4%, and the cohesive force increased by 24.4 kpa compared with that of the plain soil. The main reason for this is that, with the addition of the fibers, the fibers were able to interweave with the soil particles. Due to the microbially generated calcium carbonate deposits, the fibers and the soil particles formed a colloid and, with the application of load fibers, the soil particles were able to interweave more closely; thus, the porosity of the specimen was reduced and the compactness was increased. This formed a stable three-dimensional soil network structure, in which the frictional resistance and occlusion between the soil particles and fibers were more obvious, thus limiting the deformation of the specimen and enhancing its cohesion. When the fiber content is too high, the fibers tend to overlap and accumulate in the soil, which means that the soil cannot be compacted. This encroaches on the space available for microbial colonization and affects the deposition of calcium carbonate, meaning that the strength of the specimen is actually reduced. The internal friction angle of the reinforced graph increased by 2.2°~6.4° compared with that of the plain soil. This indicates that the incorporation of fibers can improve the internal friction angle of the cured soil. This is due to the deposition of microbially generated calcium carbonate and the surface roughness of coconut fibers which increase the frictional resistance between the soil particles, resulting in an increase in the internal friction angle. When there is too much fiber admixture and when the amount of calcium carbonate generation decreases, the frictional resistance decreases. The fibers form a mass and the bite force effect of soil particles is decreased. The weak surface of the soil structure weakens the interfacial action of the reinforced soil and the action of the soil skeleton particles, resulting in a decrease in the internal friction angle.

3.1.3. Analysis of the Deformation Modulus and Reinforcement Effect

The modulus of deformation is an important physical quantity in describing the deformation characteristics of soil. It reflects the extent of the specimen's ability to resist deformation: the larger the value, the smaller the possibility of damage under the same deformation conditions. The modulus of deformation for the CU test is usually taken as half of the difference between the principal stress at the point of damage and the ratio of its corresponding axial strain [45]. The relationship between the deformation modulus and the confining pressure for different fiber doping values is shown in Figure 13 below.

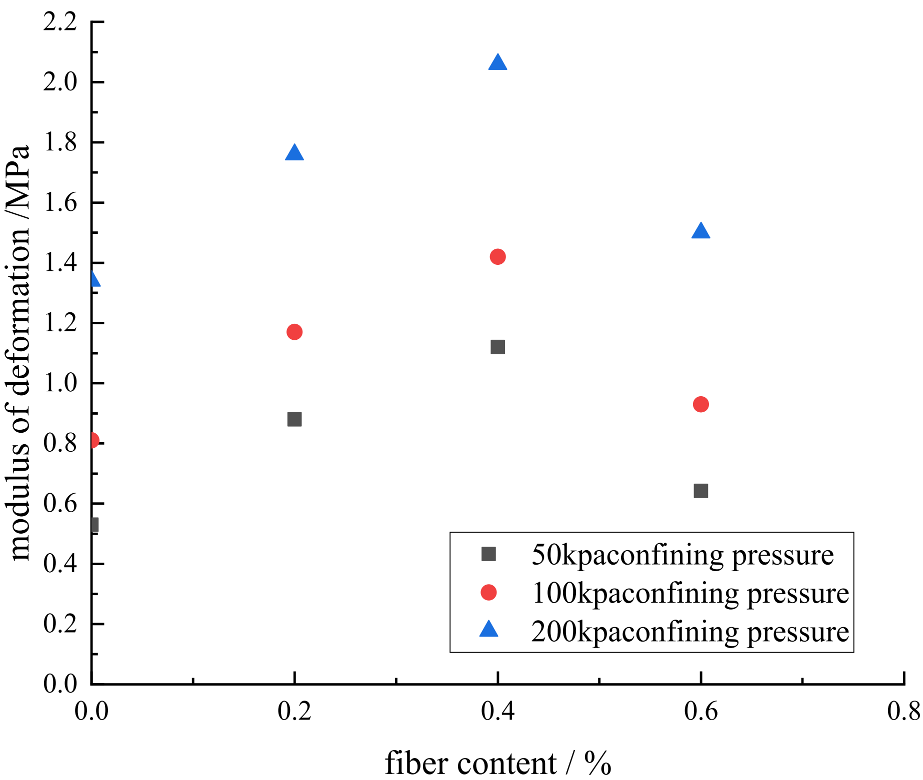

Figure 13. Deformation modulus of each sample.

When the fiber content was the same, the deformation modulus increased with the increase in the confining pressure. The main reasons for this are as follows: the greater the confining pressure, the greater the compression in the consolidation process; the greater the relative density, the stronger the soil particles, the stronger the interlocking effect between the soil particles and the calcium carbonate and fibers; the stronger the shear deformation resistance, the smaller the strain required and the greater the deformation modulus. The deformation modulus of the reinforced cured soil increases with the amount of fiber dosing and then decreases. We take the confining pressure of 100 kpa as an example; when the fiber content increased from 0 to 0.4%, the deformation modulus increased from 0.81 MPa to 1.418 MPa, amounting to an increase of 75%; however, when the fiber content increased to 0.6%, the deformation modulus decreased to 0.928 MPa. This shows that the addition of fibers can improve the plasticity of the soil, thus improving its deformation resistance.

In order to analyze the effect of the coconut shell fibers on the reinforcing effect of microbially cured clayey soil, the coefficient of the fiber-reinforcing effect was introduced [46,47] as follows:

$$R = \frac{(\sigma_1 - \sigma_3)f}{(\sigma_1 - \sigma_3)s}, \tag{6}$$

where R is the reinforcement effect factor; $(\sigma_1 - \sigma_3)f$ is the deviatoric stress when the fiber-reinforced cured soil is damaged; and $(\sigma_1 - \sigma_3)s$ is the main deviatoric stress when the microbial cured soil is damaged, as shown in Table 3.

Table 3. Reinforcement effect coefficients of microbial-solidified soil under different fiber contents.

Specimen Type	Reinforcement Effect Factor, *R*		
	50 kPa	**100 kPa**	**200 kPa**
Plain soil	1.00	1.00	1.00
Fiber content 0.2%	1.65	1.45	1.49
Fiber content 0.4%	2.11	1.76	1.53
Fiber content 0.6%	1.21	1.15	1.12

It can be seen that the reinforcement effect coefficients of the fiber soil were greater than 1.0 under different confining pressures, which indicates that the fibers can effectively improve the shear strength of soil and restrain soil deformation after they are incorporated into cured soil. The reinforcement effect coefficient of the fiber-reinforced cured soil with a 0.4% fiber admixture was the largest under different confining pressures. This indicates that the reinforcement effect was the best when the fiber admixture was 0.4%, which is consistent with the results of the stress–strain curve.

3.2. Determination of Calcium Carbonate Content

In this study, the amount of calcium carbonate produced was closely related to the curing effect; therefore, the measurement of the calcium carbonate content in the cured sample reflects the progress of the MICP technology. The amount of calcium carbonate generated in the specimens treated with the MICP technique at different fiber admixtures (for example, in the case of a 200 confining pressure) is shown in Figure 14 below. With the increase in the fiber admixture, the amount of calcium carbonate generated tended to increase first and then decrease. This is mainly because the addition of fiber to the mix provides a good attachment point for bacteria during the mixing process, and there are more areas for microorganisms to colonize after entering the soil body. However, the addition of fiber in excess crowds the living space of microorganisms, leading to a lower amount of calcium carbonate being generated. When the calcium carbonate production of the specimen with a 0.6% fiber content was higher than that of the cured, reinforced soil with a 0.2% fiber content, its peak shear strength was lower than that of the sample with a 0.2% fiber content. This was probably because the fiber content was too high. When the fiber content is too high, it easily forms clumps during the mixing process, which reduces the friction between the soil particles. This can easily lead to an uneven fiber distribution, which affects the migration and colonization of microorganisms and leads the calcium carbonate generated inside the specimen to become unevenly distributed; thus, the variability in the local curing is too large. This renders the curing effect unsatisfactory.

This shows that the calcium carbonate content is not the only factor that determines the mechanical properties of a sample.

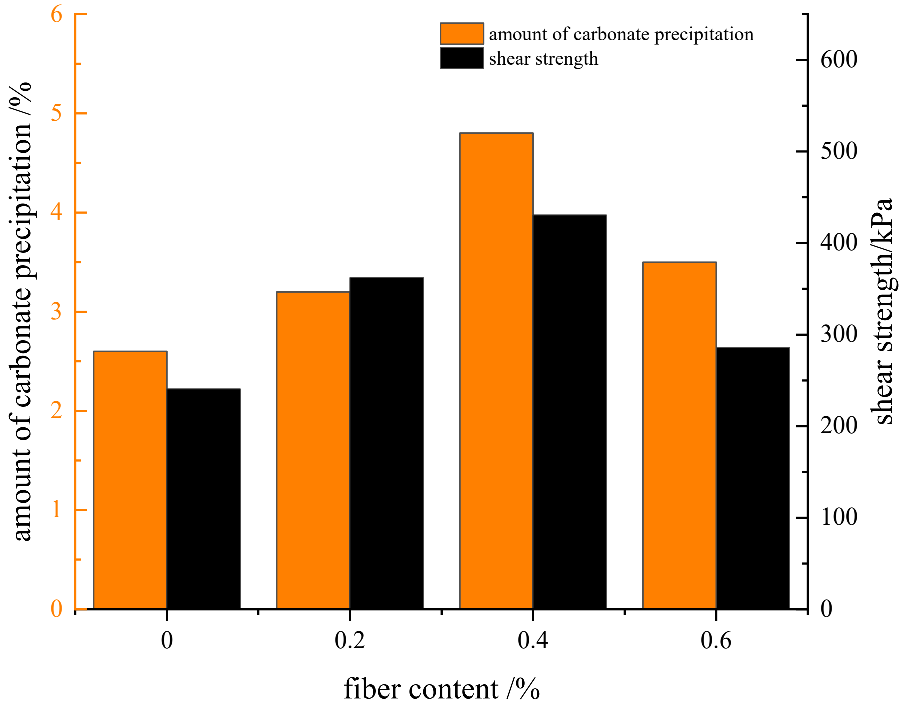

Figure 14. Calcium carbonate production with different fiber contents.

3.3. Disintegration Characteristics

Once the reinforced clayey soil that was treated with MICP was completely immersed in the water, the test entered the wetting stage. Due to the existence of pores on the surface of the specimen, the water penetrated through the micro-cracks on its surface. The pore gas was then discharged, producing a large number of bubbles. With the progression of the immersion time, the specimen entered the softening stage, in which it gradually began to produce inward cracks; the soil particles and fibers gradually separated, and the fibers inside the specimen were slowly revealed. The disintegration rate during this stage was slow. With the further passage of time, the specimen began to disintegrate rapidly, entering the disintegration stage. At this point, the soil particles and fibers separated rapidly, the whole of the outer part of the soil and fibers began to fall off, and the water quickly became turbid. The disintegration phenomenon was violent. After the disintegration of the soil, the remaining soil and fibers of the specimen formed a cone-shaped pile in the disintegration box and the disintegration volume of the specimen no longer increased—only a small number of soil particles were scattered. After this, the specimen entered the stabilization stage. It should be noted that the wetting stage and the softening stage of the MICP-treated loess specimen, without reinforcement, were basically the same as those of the reinforced specimen; however, its disintegration stage was more rapid and it was completely disintegrated in a shorter amount of time.

Figure 15 shows the disintegration curves of different fiber-doped viscous soil specimens. With the increase in the water immersion time, the fiber-free specimens began to disintegrate rapidly and the disintegration rate reached 90.7% between 1.5 min and 8 min, during a total of 10 min of water immersion. This was unlike the phenomenon observed for the plain soil specimens, whereby all the fiber-doped specimens failed to reach a 100% disintegration rate. The final disintegration rate of the reinforced soil with 0.2%, 0.4% and 0.6% fibers decreased by 13.3%, 25.6%, and 33.7%, respectively, compared with that of the plain soil, as the fiber incorporation increased from 0 to 0.6%. The decrease in the final disintegration rate was the most obvious when the fiber admixture increased from

0.4% to 0.6%. Combined with the disintegration process, the main reason for this was that, after the disintegration of the soil particles at the bottom of the specimen, the fibers were longer than the size of the gaps in the metal mesh at the bottom of the disintegration box; therefore, some fibers filled the gaps in the metal mesh, so that the soil particles could not be easily dislodged from the disintegration box. This, in turn, led to more soil residue in the disintegration box.

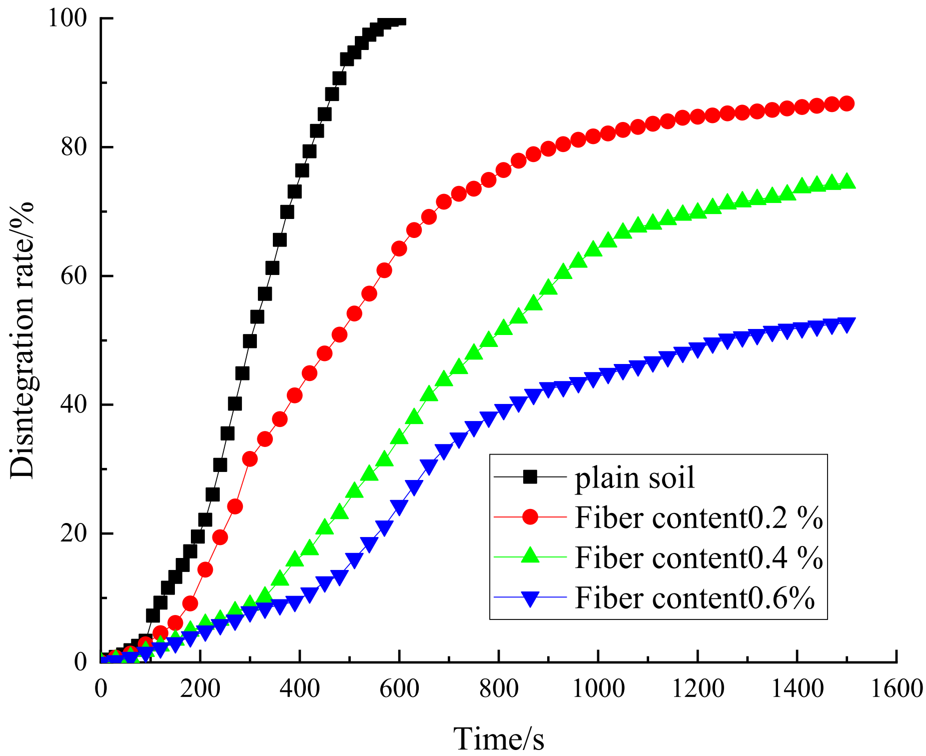

Figure 15. Effect of different coconut fiber contents on the disintegration rate.

3.4. Microstructure Analysis

To analyze the mechanism of the effect of incorporating fibers on the reinforcement of MICP, the microstructure of the fiber-reinforced, microbially cured clayey soil was observed using scanning electron microscopy. The soil mass inside the specimen after its destruction at the end of the triaxial test was taken and magnified at different magnifications, as shown in Figure 16 below. In the image that was magnified 50 times, it can be seen that the fibers are interspersed in the soil from different angles and interwoven into a network. It can also be seen that under the action of external force, some fibers are bent or there is a deformation on the surface, which, from a mechanical point of view, is beneficial to increasing the degree of fiber and soil occlusion and the contact area. It can also have a restraining effect on load-induced displacement. This reinforcing effect is further enhanced by the restraining effect of the displacement caused by the load [48,49]. When the sample is destroyed, the fiber plays a similar role as a bridge in the soil. The fiber spans the crack like a bridge and can bear a certain tensile stress, which can effectively inhibit the further development of the crack and delay the overall failure of the sample [50,51]. At a magnification of 100 times, the calcium carbonate crystal filled the space between the soil particles so that the particles were glued to each other and the overall connection between the particles was strengthened. At magnifications of 1000 and 5000 times, the calcium carbonate crystals were scaled and attached to the fiber's surface. This occurred because the fiber that was added to the soil was in the pores of the soil, and, as the amount of admixture increased, the corresponding surface area also increased. The increase in the breeding sites and the enrichment of the microorganisms further improved the curing effect, and the surface of the fibers was gradually covered by the calcium carbonate that was generated. It was found that the addition of appropriate amounts of fibers helped the curing reaction and the deposition of the calcium carbonate, and that the adhesion between the calcium carbonate and particles increased the friction between the fibers and the soil. This was conducive to improving the reinforcing effect of the soil and the strength of the sample.

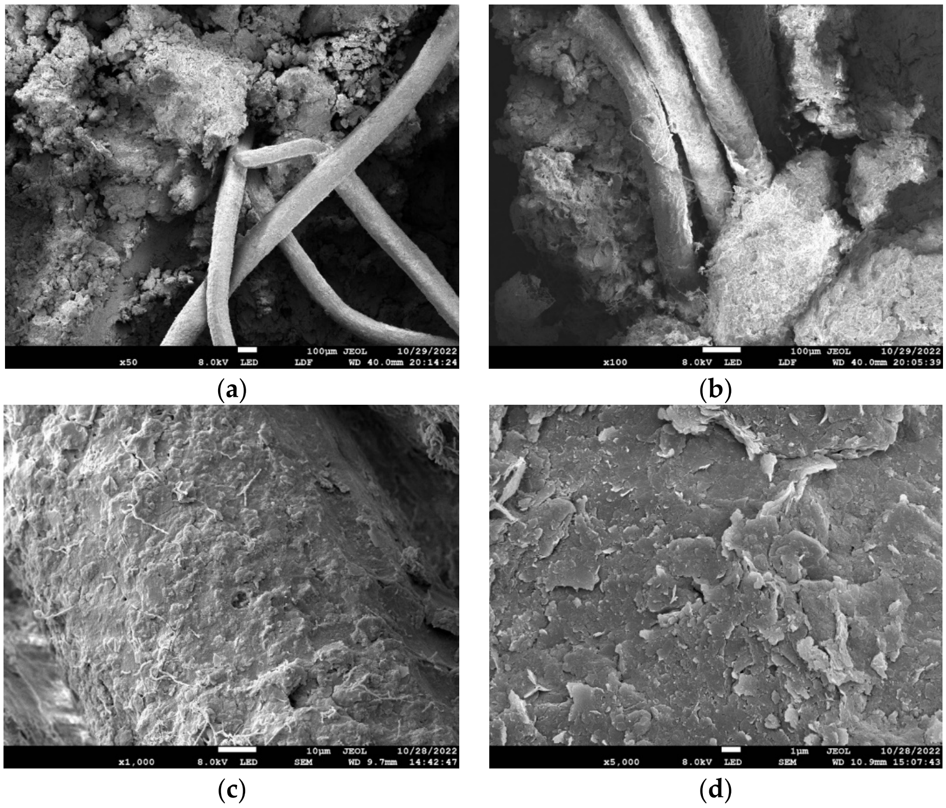

Figure 16. SEM electron microscope scan. (**a**) Magnification: 50 times; (**b**) magnification: 100 times; (**c**) magnification: 1000 times; (**d**) magnification: 5000 times.

4. Conclusions

In this paper, clayey soil was mixed and solidified, and the influence of the different fiber contents on its mechanical properties was analyzed via a triaxial shear test. The influence of the fiber content on the content of calcium carbonate was discussed. The effect of fiber reinforcement and MICP technology on the soil's water stability was studied through a disintegration test. The reinforcement mechanism of the fiber was discussed based on microscopic electron microscopy images. The following conclusions were obtained:

(1) The combination of microbial curing technology and fiber reinforcement technology can significantly improve the shear strength of clayey soil. The coupling of the two technologies has a better curing effect than the employment of a single technology. The addition of fibers alleviates the problem of brittleness in microbial solidified soil, enhancing the ductility of the soil and strengthening its deformation resistance. This is significant in improving the safety and stability of engineering structures.

(2) The fiber admixture has an important effect on the mechanical properties of microbial curing. The shear strength of the soil sample increases first and then decreases, and the optimum admixture is 0.4%. The corresponding reinforcement effect coefficient is also the largest. In current research, the internal friction angle and cohesion after the reinforcement treatment were higher than those of the plain soil; the internal friction angle increased by 6.4, and the cohesion increased by 24.4 KPa at the optimum admixture.

(3) The calcium carbonate formation and fiber content of the samples with the same fiber content increased first and then decreased. The results did not necessarily adhere to the notion that the higher the calcium carbonate content, the higher the strength of the

soil sample, indicating that the calcium carbonate content is not the only factor that determines the mechanical properties of the sample. This finding may also be related to the cementation mode of the soil samples and the distribution characteristics of the calcium carbonate.

(4) The MICP technology can significantly improve the complete disintegration time and improve water stability. The disintegration process can be divided into four stages: the wetting stage, the softening stage, the caving stage, and the disintegration stability stage. The addition of fibers can significantly improve the anti-disintegration performance of soil samples. The higher the fiber content, the slower the disintegration rate, and the stronger the anti-disintegration ability. The lowest disintegration rate of the coconut fibers was detected when the content was 0.6%. The water stability of the soil treated with both techniques was stronger than that of the sample cured without reinforcement.

(5) Scanning electron microscopy showed that the addition of fibers can provide more colonization space for microorganisms, thereby increasing the efficiency and yield of calcium carbonate sedimentation. Calcium carbonate crystals were attached to the surface of fibers and soil particles in flakes, which effectively improved the surface roughness of the soil particles, enhancing the anchoring force of the fibers in the soil and further enhancing the reinforcement effect. This suggests that MICP technology and fiber reinforcement technology complement each other.

(6) Based on the coupling of microbial mineralization technology and fiber reinforcement technology, the indoor test shows that the method has a good effect on soil solidification and improves the soil water stability. Compared with the method of only adding fiber without microorganisms, the microbiological curing technology can complement the reinforcement technology, so that the curing effect can be improved. In comparison with the study that only conducted microbial curing without adding fiber, the addition of fiber alleviated the disadvantages brought by microbial curing; this technique thus provided a new basis for soil reinforcement and the prevention of soil erosion in China. In the future, it will be necessary to carry out systematic and in-depth research on the effects, treatment process, influencing factors, and other aspects of this technique so as to lay a foundation for the practical engineering application of the proposed technical methods.

Author Contributions: W.S.: writing—original draft, resources and methodology. Q.H.: review, editing and funding acquisition. J.H.: visualization. All authors have read and agreed to the published version of the manuscript.

Funding: This research received no external funding.

Institutional Review Board Statement: Not applicable.

Informed Consent Statement: Not applicable.

Data Availability Statement: The data are displayed in the paper.

Conflicts of Interest: The authors declare no conflict of interest.

References

1. Whiffin, V.S. Microbial $CaCO_3$ Precipitation for the Production of Biocement. Ph.D. Thesis, Murdoch University, Perth, Australian, 2004.
2. Chu, J.; Ivanov, V.; Naeimi, M.; Li, B.; Stabnikov, V. Development of Microbial Geotechnology in Singapore. In Proceedings of the Geofrontiers 2011: Advances in Geotechnical Dallas: ASCE, Dallas, TX, USA, 13–16 March 2011; pp. 4070–4078.
3. Qabany, A.A.; Soga, K.; Santamarina, C. Factors affecting efficiency of microbially induced calcite precipitation. *J. Geotech. Amp. Geoenviron. Eng.* **2012**, *138*, 992–1001. [CrossRef]
4. Liu, H.L.; Ma, G.L.; Xiao, Y.; Ding, X.M.; Fang, X.W. Field test of microbial reinforced reef foundation. *Found. Treat.* **2019**, *1*, 26–31.
5. Cui, M.J.; Zheng, J.J.; Zhang, R.J.; Miao, C.X.; Zhang, J.J. Study on the effect of chemical treatment on the strength of microbial solidified sand. *Geomechanics* **2015**, *36*, 392–396. [CrossRef]

6. Cui, M.J.; Zheng, J.J.; Lai, H.J. Experimental study on the effect of particle size on the strength of microbial solidified sand. *Geomechanics* **2016**, *37*, 397–402. [CrossRef]
7. Stocks-fischer, S.; Galinat, J.K.; Bang, S.S. Microbiological precipitation of $CaCO_3$. *Soil Biol. Biochem.* **1999**, *31*, 1563–1571. [CrossRef]
8. Peng, J.; He, X.; Liu, Z.M.; Feng, Q.P.; He, J. Experimental research on influence of low temperature on MICP-treatedsoil. *Chin. J. Geotech. Eng.* **2016**, *38*, 1769–1774.
9. Wang, J.Y.; De Belie, N.; Verstraete, W. Diatomaceous earth as a protective vehicle for bacteria applied for self-healing concrete. *J. Ind. Microbiol. Biotechnol.* **2012**, *39*, 567577. [CrossRef]
10. Cheng, X.H.; Ma, Q.; Yang, Z.; Zhang, Z.Z.; Li, M. Study on dynamic response of liquefied sand foundation reinforced by microbial grouting. *J. Geotech. Eng.* **2013**, *35*, 1486–1495.
11. Chen, Y.R.; Lei, X.W.; Wei, T.Y.; Xu, J.P.; Meng, Q.S. Experimental study on solidification of reddish brown basalt residual soil by microbial induced carbonate deposition technology. *Sci. Technol. Eng.* **2017**, *17*, 120–126.
12. Xie, J.; Tang, C.S.; Liu, B.; Cheng, Q.; Yin, L.Y. Water stability improvement of clayey soil based on microbial-induced calcium carbonate deposition technology. *J. Zhejiang Univ.* **2019**, *53*, 1438–1447.
13. Xu, T.C.; Zhang, H.N.; Jia, C.Q.; Wang, G.H. Experimental study on the disintegration of loess improved by microbially induced calcium carbonate precipitation. *Silic. Bull.* **2023**, *42*, 674–681+707.
14. Liu, L.; Shen, Y.; Liu, H.L.; Chu, J. Research on the application of microbial cementation in the prevention and control of dam damage. *Geotechnics* **2016**, *37*, 3410–3416.
15. Liu, X.J.; Gao, X.; Pan, C.F. Experimental study on shear strength of cracks in MICP solidified soil sites. *J. Civ. Eng.* **2022**, *55*, 88–94+108.
16. Li, H.; Tang, C.S.; Yin, L.Y.; Liu, B.; Lu, C. Synergistic effect of MICP-FR to improve the mechanical properties and erosion resistance of calcareous sand. *J. Geotech. Eng.* **2021**, *43*, 1941–1949.
17. De Muynck, W.; Wdebrouwer, D.; De Belie, N.; Verstraete, W. Bacterial carbonate precipitation improves the durability of cementitious materials. *Cem. Con-Crete Res.* **2008**, *38*, 1005–1014. [CrossRef]
18. Yuan, X.L. Study on mechanism and theoretical model of microbial mineralization in cement-based materials. *Concrete* **2017**, *9*, 84–88.
19. Ghosh, P.; Mabdal, S.; Chattopadhyay, B.D. Use of microorganism to improve the strength of cement mortar. *Cem. Concr. Res.* **2005**, *35*, 1980–1983. [CrossRef]
20. Ding, Y.; Wei, W.B.; Pan, B.; Huang, X.L.; Liu, Z.X.; Liu, D.X. Research on statistical damage model of fiber-reinforced vegetated concrete substrates. *Chin. J. Geotech. Eng.* **2022**, *44*, 652–659.
21. Van Tittelboom, K.; De Belie, N.; De Muynck, W.; Verstraete, W. Use of bacteria to repair cracks in concrete. *Cem. Concr. Res.* **2010**, *40*, 157–166. [CrossRef]
22. Liu, J.L.; Hou, T.S.; Luo, Y.S. Experimental study on the lateral limitless compressive strength of cotton fiber reinforced soil. *J. Hydropower* **2018**, *37*, 12–21.
23. Li, L.Y.; Ma, W.D.; Xie, P.; Huang, R.L. Model test of natural coir fiber reinforced red clay foundation. *Coal Geol. Explor.* **2021**, *49*, 182–188.
24. Xu, W.; Liu, J.Z.; Zhang, J. Glass fiber reinforced cement-soil durability test study. *J. Railw. Sci. Eng.* **2021**, *18*, 104–111.
25. Pan, B.; Ding, Y.; Huang, X.L.; Gao, F.; Xu, W.N.; Liu, D.X. Palm fiber reinforced vegetation concrete triaxial test study. *J. Silic. Bull.* **2020**, *33*, 1153–1159.
26. Xiao, J.Z.; Xu, J.X.; Luo, S.R.; Zhang, K.J.; Zhang, Q.T. Effect of sisal fiber on fracture performance of recycled aggregate concrete. *J. Build. Mater.* **2023**, *26*, 587–595.
27. Qin, Z.L.; Zhou, Y.F.; Lin, S.L.; Liang, L. Effect of sisal fiber and glass powder on mechanical properties of concrete. *J. Guangxi Univ. Sci. Technol.* **2023**, *34*, 45–51.
28. Hao, J.B.; Zhang, H.; Li, G.C.; Liu, Z.Y.; Huang, J.X.; Jiang, Z.W. Strength and crack development characteristics of fly ash-sisal fiber composite improved expansive soil. *J. Railw. Sci. Eng.* **2022**, *19*, 2620–2628.
29. Zheng, J.J.; Song, Y.; Wu, C.C.; Cui, M.J. Mechanical properties of basalt fiber reinforced microbially cured sand. *J. Huazhong Univ. Sci. Technol.* **2019**, *47*, 73–78.
30. Zheng, J.J.; Song, Y.; Lai, H.J.; Cui, M.J. Experimental study on shear strength of sand reinforced by microbial solidified fiber. *J. Civ. Environ. Eng.* **2019**, *41*, 15–21.
31. Li, S.; Lei, X.W.; Liu, L.; Liu, R.Q. Experimental study on the shear strength of corn husk reinforced microbial cured silt. *Sci. Technol. Eng.* **2021**, *21*, 13837–13844.
32. Xie, J.; Tang, C.S.; Yin, L.Y.; Lu, C.; Jiang, N.J. Mechanical properties of fiber reinforced microbially cured sandy soil. *J. Geotech. Eng.* **2019**, *41*, 675–682.
33. Liang, J.L.; Zhao, J.T.; Yuan, J.; Qiu, R.K. Mechanical properties and particle shape analysis of carbon fiber microbial solidified sand. *Sci. Technol. Eng.* **2022**, *22*, 13434–13440.
34. Choi, S.G.; Wang, K.; Chu, J. Properties of biocemented, fiber reinforced sand. *Constr. Build. Mater.* **2016**, *120*, 623–629. [CrossRef]
35. Li, M.D.; Li, L.; Ogbonnaya, U. Influence of fiber addition on mechanical properties of MICP-treated sand. *J. Mater. Civ. Eng.* **2016**, *28*, 04015166. [CrossRef]

36. Cheng, G.; Wang, S.J.; Li, X.; Shen, Y.T.; Xu, C. Experimental study on microbial solidified fiber reinforced sandy cohesive purple soil. *J. Undergr. Space Eng.* **2021**, *17*, 1829–1838.
37. Lu, W.; Luo, W.; Li, D.B.; Liu, Q.L.; Liu, J.P. Study on the properties of ecological grouting materials for coconut shell fiber reinforced earthen sites. *J. Build. Mater.* **2023**, 1–12.
38. Wang, J.X.; Zuo, H.F. Coir fibre and the performance and application of coconut carbon fiber. *J. Text. Sci. Technol. Prog.* **2020**, *2*, 5–7.
39. Pan, Y.J.; Wang, Z.; Liu, Y.S. Study on the effect of pretreated coconut shell fiber on the properties of cement-based materials. *Concr. Cem. Prod.* **2022**, *5*, 61–66.
40. Yin, L.Y.; Tang, C.S.; Xie, J.; Lu, C.; Jiang, N.J.; Shi, B. Influencing factors of microbial mineralization to improve the properties of geomaterials. *Geomechanics* **2019**, *40*, 2525–2546. [CrossRef]
41. Harkes, M.P.; Paassen, L.A.V.; Booster, J.L. Fixation and distribution of bacterial activity in sand to induce carbonate precipitation for ground reinforcement. *Ecol. Eng.* **2010**, *36*, 112–117. [CrossRef]
42. Peng, J.; Tian, Y.M.; Yang, J.G. MICP reinforced coral sand test in seawater environment. *Technol. Prog. Water Conserv. Hydropower* **2019**, *39*, 58–62.
43. Song, X.L. Comparison of direct shear saturated consolidated fast shear and triaxial consolidated undrained shear tests. *Shanxi Water Conserv.* **2013**, *29*, 33–34.
44. Hu, Q.Z.; Shu, S.; Tao, G.L.; Zhang, F. Study on the strength mechanism of microbial solidified clay-bearing granite residual soil. *Sci. Technol. Eng.* **2022**, *22*, 4920–4927.
45. Gao, L.; Hu, G.H.; Chen, Y.H.; Hu, Y.J.; Gong, Y.H. Triaxial test of basalt fiber reinforced clay. *Chin. J. Geotech. Eng.* **2017**, *39*, 198–203.
46. Xu, H.Z.; Peng, Y.Q.; Zhao, Z.P.; Teng, K. Experimental study of chopped basalt fiber reinforced expansive soil. *Build. Sci.* **2012**, *28*, 44–47. [CrossRef]
47. Wang, X.Q.; Guo, M.; Hu, B. Triaxial test study of geogrid-reinforced expansive soil. *Geotech. Mech.* **2011**, *32*, 1649–1653. [CrossRef]
48. Li, J.; Tang, C.S.; Wang, D.Y.; Shi, B.; Pei, X.J. Study on interface strength of corrugated fiber reinforced soil based on single fiber pulling test. *Chin. J. Geotech. Eng.* **2014**, *36*, 1696–1704.
49. Tang, C.S.; Shi, B.; Gao, W.; Cai, Y.; Liu, J. Strength and mechanical behavior of short polypropylene fiber reinforced and cement stabilized clayey soil. *Geotext. Geomembr.* **2007**, *25*, 194–202. [CrossRef]
50. Wang, D.Y.; Tang, C.S.; Li, J.; Liu, B.S.; Tang, W.; Zhu, W. Shear strength characteristics of fiber reinforced unsaturated clay. *J. Geotech. Eng.* **2013**, *35*, 1933–1940.
51. Tang, C.S.; Wang, D.Y.; Cui, Y.J.; Shi, B.; Li, J. Tensile strength of fiber reinforced soil. *J. Mater. Civ. Eng.* **2016**, *28*, 04016031. [CrossRef]